Journal of Fluorescence (2019) 29:1249–1255
https://doi.org/10.1007/s10895-019-02439-4

ORIGINAL ARTICLE

Photoluminescence Studies of Rare Earth Doped Apatite Structured Phosphors

Pailendra Kumar Sahu[1] · **Meera Ramrakhiani**[2] · **Sadhana Agrawal**[1]

Received: 1 June 2019 / Accepted: 10 September 2019 / Published online: 15 October 2019

Abstract

We developed novel phosphors based on $Y_6Ba_4(SiO_4)_6F_2$(YBSF) apatite doped with Dy^{3+}. Phosphors with different doping concentrations of Dy^{3+} were prepared and their morphological, structural and spectral properties were analyzed. XRD pattern confirms the formation of $Y_6Ba_4(SiO_4)_6F_2$ apatite structured phosphors with space group $P6_3/m$ and Debye scherrer formula gives the average crystalline size 33.4 nm. The morphological and topographical studies were done by FESEM and HRTEM analysis. EDX spectra show presence of all initial reactants in the final product. Photoluminescence spectra show two prominent peaks at 487 nm and 573 nm corresponding to magnetic dipole transitions ($^4F_{9/2} \rightarrow {}^6H_{15/2}$) and electric dipole transitions ($^4F_{9/2} \rightarrow {}^6H_{13/2}$) for 350 nm excitation wavelength. The chromaticity coordinate of the prepared phosphors was found to be in the region of near white light which shows that prepared phosphor are potential single phased phosphor for white light emitting diodes.

Keywords Apatite · Luminescence · Hexagonal · Phosphors · Color correlated temperature

Introduction

Earlier incandescent bulb and fluorescent lamps were in vogue. Studies have showed that incandescent bulb and fluorescent lamps have adverse effect on environment [1–3]. Researchers are much more focused on the development of white light emitting diodes (w-LEDs) which has certain properties like mercury free environment, more operational life and low energy consumption [4–7]. A commercial w-LEDs available today is a combination of InGaN blue chip and a YAG:Ce^{3+} yellow phosphor [8, 9]. This method of obtaining w-LEDs has certain shortcomings like low color rendering index (CRI) and high correlated color temperature (CCT) because of insufficient red emission [10, 11]. Alternatively another method was adopted by combining near ultraviolet (NUV) LED chips with tricolour (Red, Green & Blue) phosphors to overcome the problem of low color rendering Index (CRI) and high correlated color temperature (CCT). But its high cost and self-adsorption among the phosphors affected its luminous efficiency [12]. The present paper reports study on YBSF phosphors which can be used as single-phased NUV excited white light phosphor [13, 14].

Apatite group of compound has hexagonal crystal structure with space group $P6_3/m$ having general structural formula $A(I)_{10\text{-}x}A(II)_x(ZO4)_6Q_2$. A(I) and A(II) represents two different crystallographic (cationic) sites, one is 4f site with nine-fold coordinate site and another is 6 h site with seven fold coordinate site [15, 16]. It is generally occupied by alkali, alkaline-earth or rare earth atoms. Z site is occupied by phosphorous, vanadium, silicon, boron, germanium etc. and Q is anion site occupied by bromide, hydroxyl, chlorine, fluoride etc. [13, 17, 18].

In the present paper YBSF apatite phosphor are doped with Dy, a well known and extensively studied material from rare earth family. When dysprosium is combined with YBSF apatite phosphors materials it showed emission in blue and yellow region of visible spectrum due to $^4F_{9/2} \rightarrow {}^6H_{9/2}$ and $^4F_{9/2} \rightarrow {}^6H_{13/2}$ transitions [19–21].

Experimental

Novel apatite compound with formula $Y_6Ba_4(SiO_4)_6F_2{:}xDy^{3+}$($x = 0,0.4,0.6,1$ mol%) having different doping concentrations were prepared by conventional solid state reaction

---

✉ Sadhana Agrawal
sagrawal.phy@nitrr.ac.in

[1] Department of Physics, National Institute of Technology Raipur, Raipur 492010, India

[2] Department of Post Graduate studies and Research in Physics and Electronics, Rani Durgavati University, Jabalpur, India

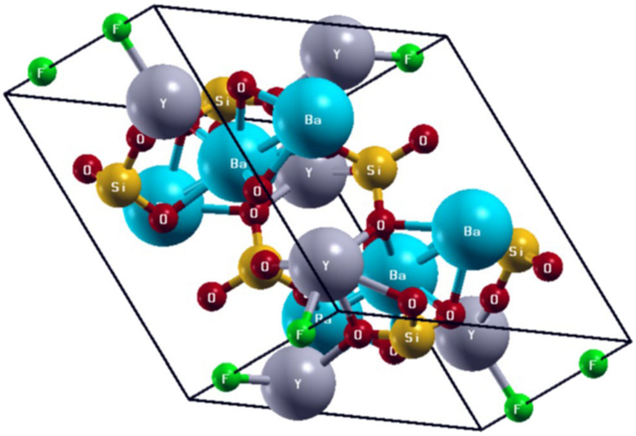

Fig. 1 Representation of $Y_6Ba_4(SiO_4)_6F_2$

method. Starting material Y_2O_3, $BaCO_3$, SiO_2, BaF_2 and Dy_2O_3 were taken in stiochiometric ratio and 50 mol% excess amount of BaF_2 was added to prevent the loss of flourine [22, 23]. Further, the mixture was ground in an agate mortar and pestle for 40 min and placed in an alumina crucible and kept in a muffle furnace at 1200 °C for 4 h with a heating rate of 5 °C per minute. The samples were cooled naturally. The samples were crushed and again ground for 40 min in an agate mortar and pestle. The samples were calcined at 1500 °C for 5 h with a heating rate of 5 °C per minute and muffle cooled. The obtained products were further ground to obtain the YBSF apatite phosphor in a fine powder form.

$$\mathbf{BaCO_3 \rightarrow BaO + CO_2} \uparrow$$

$$\mathbf{3Y_2O_3 + BaF_2 + 3BaO + 6SiO_2 \xrightarrow{Dy_2O_3} Y_6Ba_4(SiO_4)_6F_2{:}Dy^{3+}}$$

Result and Discussion

XRD

3 kW PANalytical -XPERT powder X-ray diffractometer was used for determining the phase structure of the prepared phosphors with CuKα(λ = 0.15405 nm) at generator voltage of 40 kV and tube current of 30 mA. Average crystalline size of the prepared sample was calculated by using debye-scherrer formula (Eq. 1) and was found to be 33.4 nm for YBSF [24].

Table 1 Structure parameters and ionic radii for a given CNs of Y^{3+}, Ba^{2+} Dy^{3+} ions

Ion	Sites	Symmetry	Ionic Radius(Å) CN = 9	Ionic Radius(Å) CN = 7
Y^{3+}	4f/6 h	C_3/C_s	1.075	0.96
Ba^{2+}			1.47	1.38
Dy^{3+}			1.083	0.97

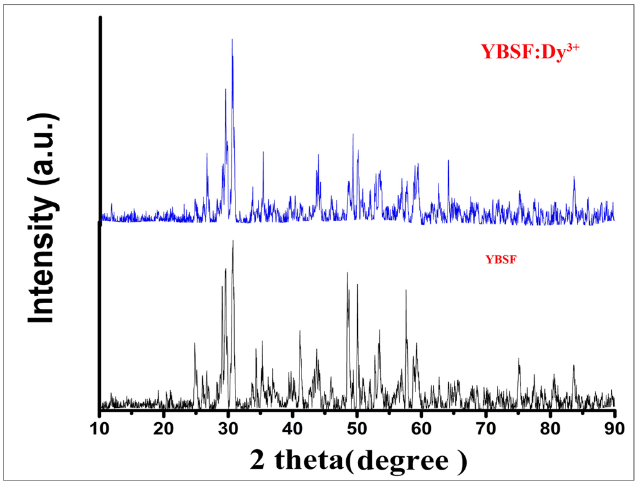

Fig. 2 X-Ray Diffraction pattern of $Y_6Ba_4(SiO_4)_6F_2$ and $Y_6Ba_4(SiO_4)_6F_2{:}Dy^{3+}$

$$\tau = \frac{k\lambda}{\beta\cos\theta} \qquad (1)$$

Where τ is average crystalline size, k = 0.9 (dimensionless shape factor), β = 0.2674 is FWHM in radians, θ = 0.0043 is bragg angle in radians and λ is wavelength of X-ray used.

Figure 1 shows the structural representation of YBSF apatite phosphors.

YBSF belongs to apatite structured compound (Fig. 1), having hexagonal crystal system with space group $P6_3/m$. YBSF provides two non equivalent crystallographic cationic sites (4f and 6 h). 4f cationic site has C_3 symmetry with nine co-ordination (Y^{3+}/Ba^{2+}(I)) and 6 h cationic site has C_s symmetry with seven co-ordination (Y^{3+}/Ba^{2+}(II)).Y^{3+} and Ba^{2+} placed in 4f site (Y^{3+}/Ba^{2+}(I)) has occupancy percentage of 75% and 25% where as that in 6 h site (Y^{3+}/Ba^{2+}(II)) are 37.5% and 62.5% respectively. Since the ionic radii of Dy^{3+} in nine coordinate and that of Y^{3+} in seven coordinate are almost similar (Table 1) hence Dy^{3+} randomly occupy the 4f site (Y^{3+}(I)) with nine-coordination and 6 h (Y^{3+}(II)) site with seven coordination. The Charge balance on Y^{3+} and Dy^{3+} are same which also favours the Dy^{3+} to occupy Y^{3+} site [25–27].

XRD pattern of the prepared phosphors are shown in Fig. 2. X-ray diffarction pattern confirms the crystalline nature of the prepared YBSF:Dy^{3+} phosphors due to presence of sharp peaks. X-ray diffraction peaks were analyzed which confirms the formation of YBSF:Dy^{3+} apatite with hexagonal crystal structure having space group $P6_3/m$. The XRD pattern was indexed with a reference pattern $La_6Ba_4(SiO_4)_6F_2$ having JCPDS card number 98–017-0852 [28]. The doping of Dy^{3+} does not cause any considerable change in the host crystal

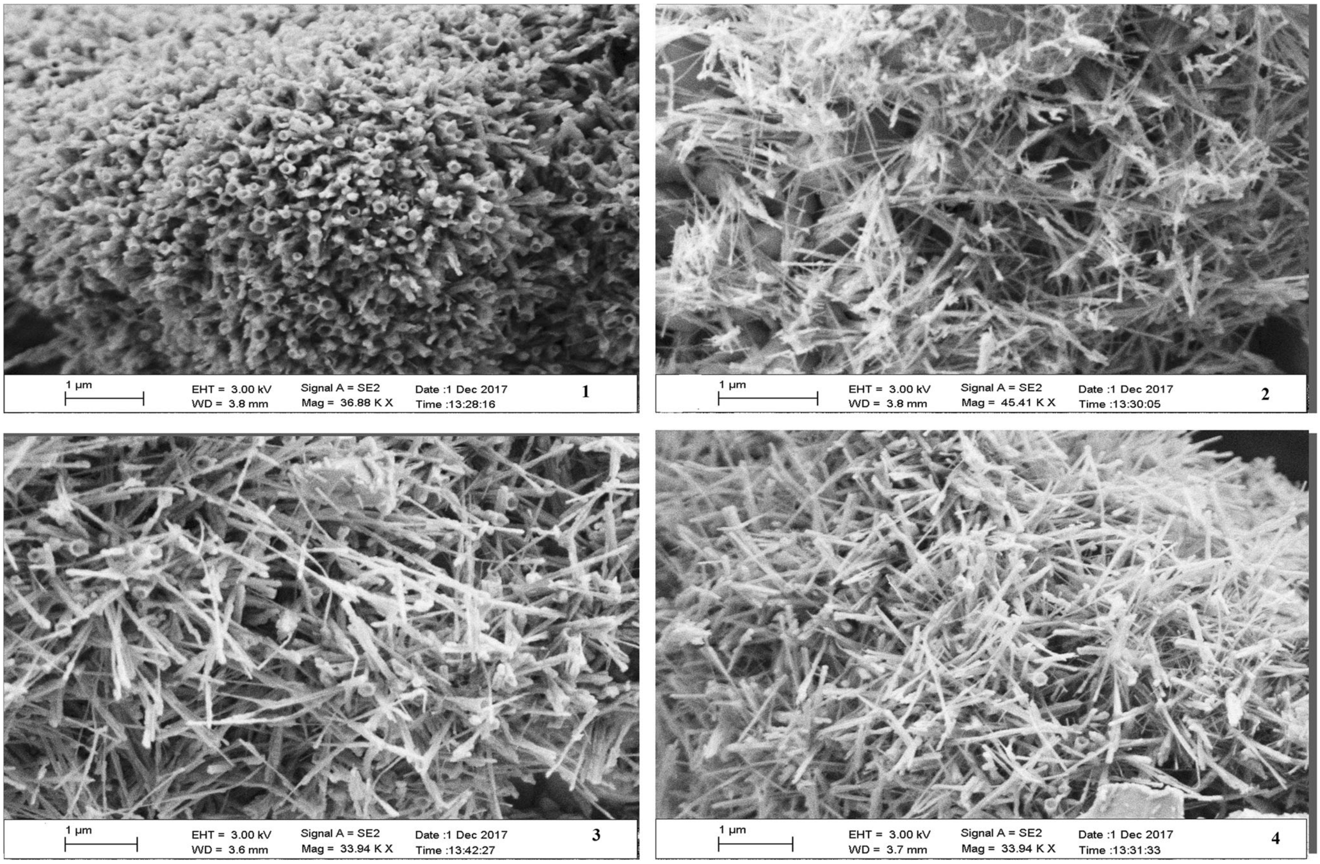

Fig. 3 FE-SEM images of YBSF (labelled 1 & 2) and YBSF:0.6Dy^{3+} (labelled 3 & 4) Phosphors on a scale of 1 μm

Fig. 4 EDX spectra of (**a**) Undoped YBSF and (**b**) YBSF:0.6Dy^{3+}

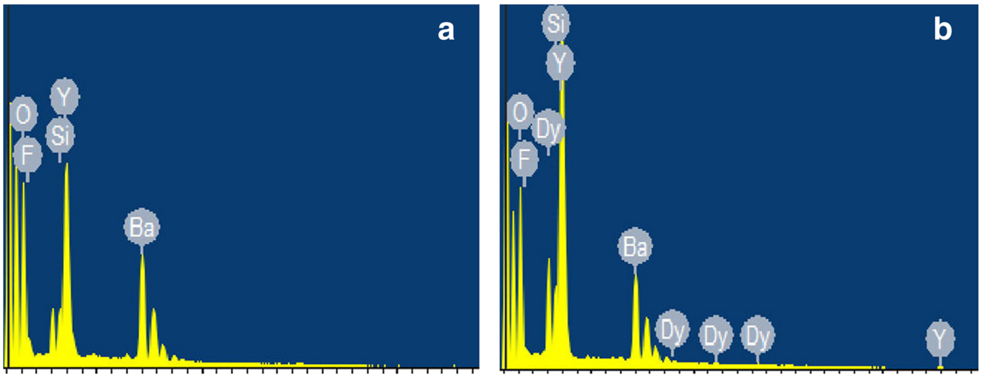

Fig. 5 HR-TEM Image of (**a**) YBSF and (**b**) YBSF:0.6Dy^{3+} phosphors

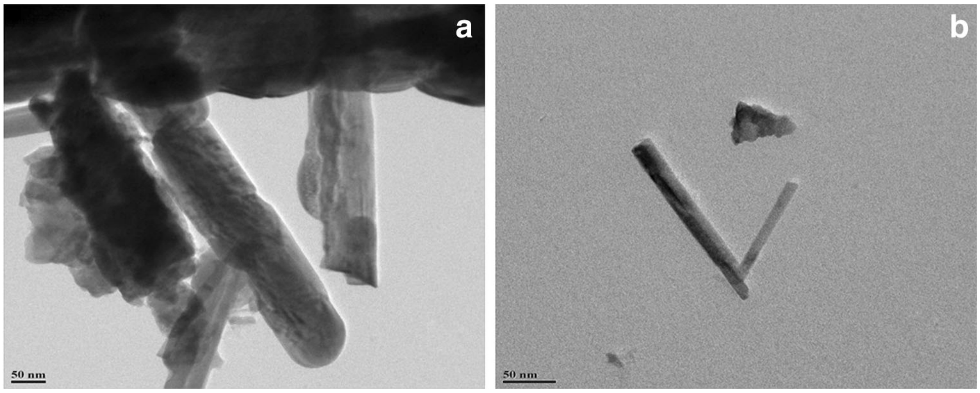

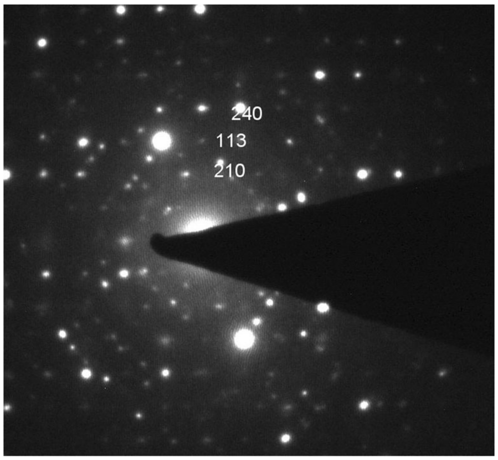

Fig. 6 SAED image YBSF:0.6Dy^{3+}

lattice which confirms that Dy^{3+} ions are perfectly incorporated in the host crystal. The value of lattice parameters were calculated for different peaks obtained in X-ray diffraction pattern by analytical method and the value of a = b = 8.47 Å and c = 10.88 Å was found which confirm the Hexagonal structure of the synthesied phosphors. The unit cell volume and axial ratio was found to be 675.96 Å ^{3} and 1.28 Å respectively.

FE-SEM and HR-TEM

Figure 3 show the FE-SEM (Field emission scanning electron microscope) images of the prepared YBSF:Dy^{3+} phosphors recorded with Zeiss-oxford SEM analyzer. FESEM images show irregular shaped pipe like structure with average particle size of 841 nm and average diameter of pipe was found to be 170.6 nm.

Energy dispersive X-ray (EDX) spectra of the prepared YBSF and YBSF:0.6Dy^{3+} apatite phosphors shows the presence of all initial reactants as shown in Fig. 4.

HR-Transmission electron microscope (TEM) micrographs were recorded with the help of TEM analyzer Hitachi H-600 at 200 kV.TEM images of the prepared phosphors are in good agreement with the images recorded with FESEM (Fig. 5). Average particle size of prepared phosphors was found to be 165.5 nm.

Selected area electron diffraction (SAED) image of the prepared YBSF:Dy phosphors were obtained (Fig. 6) and is in good agreement with the recorded X-ray diffraction pattern and shows the formation of polycrystalline material. Interplanar spacing (d-value) calculated from the SAED pattern for the first three rings are 3.23Å, 2.18Å and 1.60Å respectively which corresponds to (210), (113) and (240) planes of the hexagonal crystal structure of YBSF:Dy^{3+}.

Photoluminescence Study

Photoluminescence study of the prepared sample was carried out using a spectrofluorophotometer (RF-5301PC shimadzu). PL emission spectra ($\lambda_{ex} = 350$ nm) of $Y_6Ba_4(SiO_4)_6F_2$:xDy^{3+} (x = 0,0.4.0.6 & 1 mol%) is shown in Fig. 7. When the prepared sample was excited by 350 nm light it gives different emission peaks at 487 nm, 573 nm. The Photoluminescence excitation

Fig. 7 Photoluminescence Emission spectra of YBSF:xDy^{3+}(x = 0.4,0.6 &1 mol%).Inset shows concentration Quenching

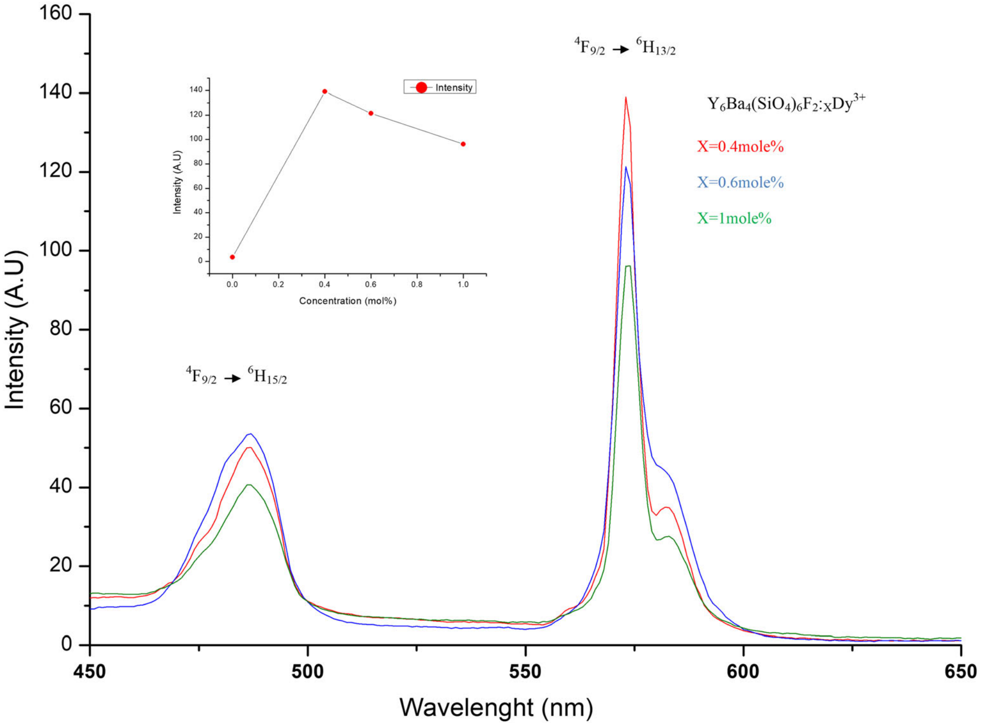

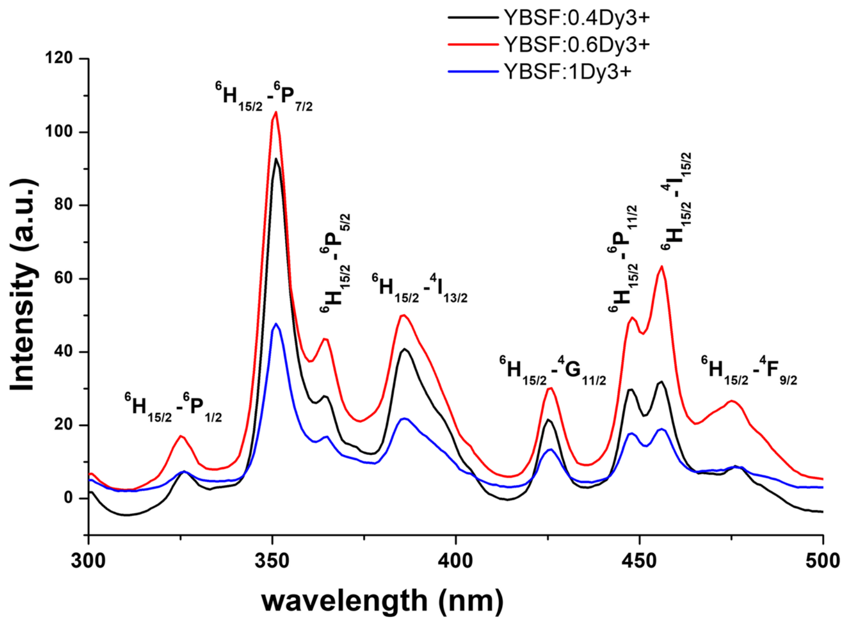

Fig. 8 Photoluminescence Excitation spectra of YBSF:xDy^{3+}(x = 0.4,0.6 &1 mol%)

(PLE) spectrum of $Y_6Ba_4(SiO_4)_6F_2{:}Dy^{3+}$ (X = 0.4,0.6&1 mol%) monitored by 574 nm (λ_{em}) is shown in Fig. 8.

In PLE spectrum when the sample is subjected to light of wavelength 574 nm several excitation peaks are observed which is due to the transition of Dy^{3+} from ground state to excited state of Dy^{3+} as shown in Fig. 9 and Tables 2 and 3.

When 350 nm excitation wavelength was used we got two emission peak located at 487 nm and 573 nm due to $^4F_{9/2} \rightarrow {}^6H_{15/2}$ and $^4F_{9/2} \rightarrow {}^6H_{13/2}$ transitions of Dy^{3+} respectively [29]. The emission intensity increases with increasing concentration of Dy^{3+} and reaches a maximum emission intensity for 0.6 mol%. On further increasing the Dy^{3+} concentration the emission intensity starts decreasing as shown in Fig. 7 (Inset). By using Blasse equation we can find the crystal distance Rc between Dy^{3+} ions for investigating the concentration quenching phenomenon [30].

$$\textit{Blasse equation}: -Rc = 2\left[\frac{3V}{4\pi XcN}\right]^{\frac{1}{3}} \tag{2}$$

In the above equation V denotes volume of of unit cell, Xc and N represents critical concentration and number of host sites which can be occupied by dopant. On substituting the values of V = 675.96Å, Xc =0.6 mol and $N = 10$ for the prepared phosphor the critical distance Rc was found to be 5.99Å. The critical distance value shows that electric multipolar transition will dominate since Rc is greater than 5Å [31].

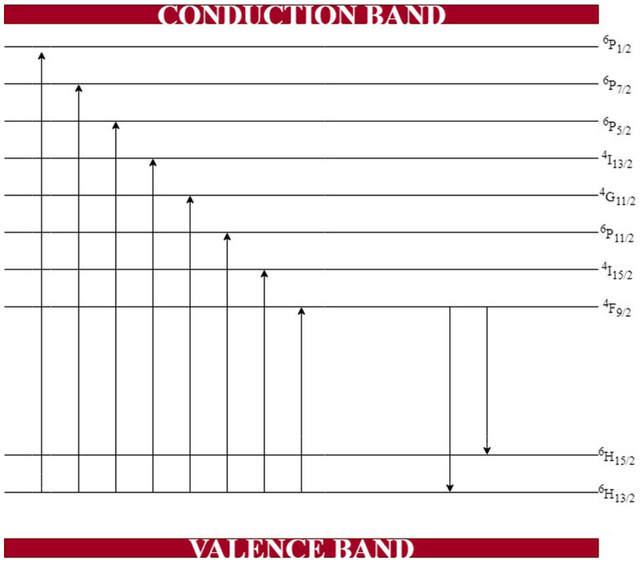

Fig. 9 Energy level transition diagram for YBSF:Dy^{3+} system

Table 2 Photoluminescence Excitation spectra transition of YBSF:Dy^{3+} Phosphors

S.No	Peak position(nm)	Transition
1	325	$^6H_{15/2}$ -$^6P_{1/2}$
2	351	$^6H_{15/2}$ -$^6P_{7/2}$
3	364	$^6H_{15/2}$ -$^6P_{5/2}$
4	385	$^6H_{15/2}$ -$^4I_{13/2}$
5	425	$^6H_{15/2}$ -$^4G_{11/2}$
6	447	$^6H_{15/2}$ -$^6P_{11/2}$
7	456	$^6H_{15/2}$ -$^4I_{15/2}$
8	476	$^6H_{15/2}$ -$^4F_{9/2}$

Table 3 Photoluminescence Emission spectra transition of YBSF:Dy^{3+} Phosphors

S.No	Peak position	Transition	Transition type
1	487	$^4F_{9/2} \rightarrow {}^6H_{15/2}$	Magnetic dipole transition
2	573	$^4F_{9/2} \rightarrow {}^6H_{13/2}$	Electric dipoleTransition

Table 4 CIE coordinates and CCT of YBSF:Dy^{3+} phosphors

S.No	Sample	X	Y	CCT(Kelvin)
1	YBSF:0.4Dy^{3+}	0.313	0.351	6344
2	YBSF:0.6Dy^{3+}	0.328	0.361	5672
3	YBSF:1Dy^{3+}	0.305	0.331	6905

CIE and Color Correlated Temperature

International commission on Illumination (CIE) chromaticity coordinate of $Y_6Ba_4(SiO_4)_6F_2$:Dy phosphors is estimated from the photoluminescence emission spectra. Figure 10 shows the CIE coordinates. Chromaticity coordinate of YBSF:Dy phosphors lies near white light region and no significant variation in chromaticity coordinate (Table 4) is observed on changing the doping of dysprosium on the prepared phosphors. The color correlated temperature (CCT) of as prepared phosphors was calculated by using polynomial formula given by McCamy's (Eq. 3) [32].

$$\mathrm{CCT(x,y)} = 449n^3 + 3525\mathrm{n}^2 + 6823.3n + 5520.33 \qquad (3)$$

Where $\mathrm{n} = \frac{x-0.332}{y-0.1858.}$

The chromaticity coordinates of an ideal white light is (X,Y) = (0.33,0.33).The prepared phosphors shows chromaticity coordinates close to (X,Y) = (0.33,0.33) as shown in Fig.10. Color correlated temperature confirms cool white light and the value for daylight is in the range of 5000 K–6500 K [33]. Our prepared phosphors is in good agreement with the daylight color temperature as shown in Table 4.

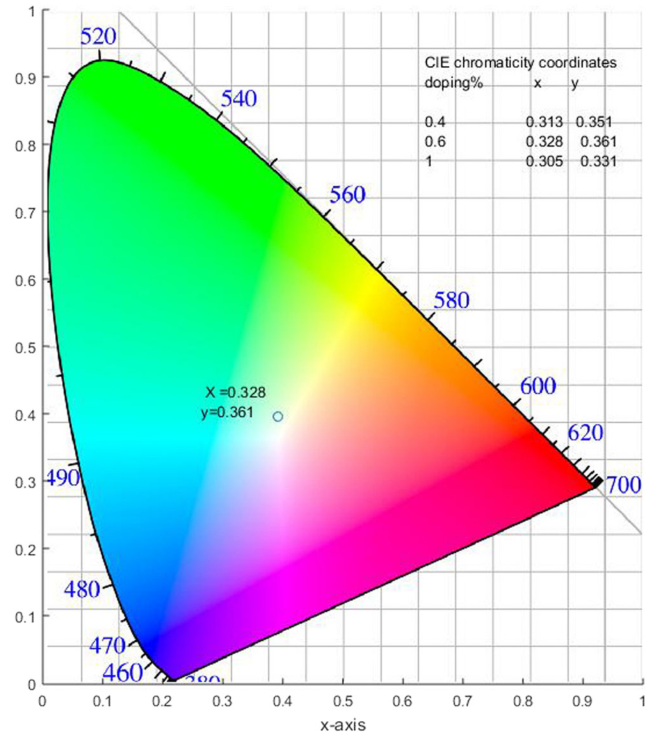

Fig. 10 CIE chromaticity graph of YBSF:Dy^{3+} Phosphors

Conclusion

A novel apatite structured $Y_6Ba_4(SiO_4)_6F_2$ was successfully synthesized via solid state reaction method. X-ray Diffraction pattern confirms the Apatite structure of $Y_6Ba_4(SiO_4)_6F_2$. SAED confirms that the prepared is polycrystalline in nature. SEM and TEM images shows similar pipe like structure. Photoluminescence (PL) Excitation and Emission spectra are obtained and concentration quenching is achieved at 0.6 mol%. PL emission spectra under 350 nm excitation wavelength was used for the calculation of CIE coordinates. CIE coordinates of the prepared phosphors is white light region. The prepared phosphors can be a potential candidate for the generation of white light for a single Host.

References

1. Kim SH, Lee HJ, Kim KP, Yoo JS (2006) Spectral dependency of Eu 2 + −activated silicate phosphors on the composition for LED application. Korean J Chem Eng 23(4):669–671
2. Romero-sandoval MR, Martinez-Martinez MT, Garcia CR, Hirata-flores GA (2016) Effect of strontium concentration on the luminescent properties of $(Ba_{1-x}Sr_x)_2SiO_4$:Eu_{2+} prepared by pressure-assisted combustion-synthesis. Int J Eng Res Sci 3:126–135
3. Chiang C, Fang Y, Lin H, Chu S (2016) Photoluminescence properties and thermal stability of samarium-doped barium phosphate phosphors. Ceram Int:0–1
4. Kemere M, Sperga J, Rogulis U, Krieke G, Grube J (2017) Luminescence properties of Eu, RE3 þ (RE ¼ Dy, Sm, Tb) co-doped oxy fluoride glasses and glass – ceramics. J Lumin 181:25–30
5. Khaidukov NM, Kirm M, Feldbach E, Mägi H, Nagirnyi V, Tõldsepp E, Vielhauer S, Jüstel T, Jansen T, Makhov VN (2017) Luminescence properties of silicate apatite phosphors M2La8Si6O26:Eu (M = Mg, Ca, Sr). J Lumin 191:51–55
6. Kumar V, Pandey A, Ntwaeaborwa OM, Dutta V, Swart HC (2017) Structural and luminescence properties of Eu3+/Dy3+embedded sodium silicate glass for multicolour emission. J Alloys Compd 708:922–931
7. Najar A, Omi H, Tawara T (2014) Scandium effect on the luminescence of Er-Sc silicates prepared from multi-nanolayer films, pp 1–6

8. Sakirzanovas S, Katelnikovas A, Bettentrup H, Kareiva A, Jüstel T (2011) Synthesis and photoluminescence properties of Sm3-doped LaMgB5O10and GdMgB5O10. J Lumin 131(7):1525–1529
9. Smet PF, Korthout K, Van Haecke JE, Poelman D (2008) Using rare earth doped thiosilicate phosphors in white light emitting LEDs: towards low colour temperature and high colour rendering. Mater Sci Eng B 146:264–268
10. Birkel A, Denault KA, George NC, Doll CE, Héry B, Mikhailovsky AA, Birkel CS, Hong BC, Seshadri R (2012) Rapid microwave preparation of highly efficient Ce 3+−substituted garnet phosphors for solid state white lighting. Chem Mater 24(6):1198–1204
11. K. Van Den Eeckhout, D. Poelman, and P. F. Smet (2013) "Persistent luminescence in non-Eu2+−doped compounds: a review," 2789–2818
12. Mao ZY, Wang DJ, Lu QF, Yu WH, Yuan ZH (2009) Tunable single-doped single-host full-color-emitting LaAlO3:Eu phosphor via valence state-controlled means. Chem Commun (3):346–348
13. Wang J, Lin H, Huang Q, Xiao G, Xu J, Wang B, Hu T, Wang Y (2017) Structure and luminescence behavior of a single-ion activated single-phased Ba2Y3(SiO4)3F:Eu white-light phosphor. J Mater Chem C 5(7):1789–1797
14. Zhang XM, Li WL, Shi L, Qiao XB, Seo HJ (2010) Photoluminescence properties of blue-emitting Li4SrCa(SiO4)2: Eu2+ phosphor for solid-state lighting. Appl Phys B Lasers Opt 99(1–2):279–284
15. Boyer L, Piriou B, Carpena J, Lacout JL (2000) Study of sites occupation and chemical environment of Eu 3 1 in phosphate-silicates oxyapatites by luminescence. J Alloys Compd 311: 143–152
16. Sio B (2014) Luminescence properties and energy transfer. J Lumin 145:65–70
17. Yu R, Xue N, Wang T, Zhao Z, Wang J, Hei Z, Li M, Mi Noh H, Hyun Jeong J (2015) Photoluminescence characteristics of high thermal stable fluorosilicate apatite Ba 2 Y 3 (SiO 4) 3 F: Sm 3 þ orange-red emitting phosphor. Ceram Int 41(4):6030–6036
18. Hughes JM, Cameron M, Crowley KD (1991) Ordering of divalent cations in the apatite structure: crystal structure refinements of natural Mn- and Sr-bearing apatite. Am Mineral 76(1975):1857–1862
19. Stefani R, Rodrigues LCV, Carvalho CAA, Felinto MCFC, Brito HF, Lastusaari M, Hölsä J (2009) Persistent luminescence of Eu2+ and Dy3+doped barium aluminate (BaAl2O4:Eu2+,Dy3+) materials. Opt Mater (Amst) 31(12):1815–1818
20. Matsui K, Arima M, Kanno H (2013) Luminescence of barium aluminate phosphors activated by Eu2+ and Dy3+. Opt Mater (Amst) 35(11):1947–1951
21. Tiwari G, Brahme N, Sharma R, Bisen DP, Sao SK, Tigga S (2016) Luminescence properties of dysprosium doped di-calcium di-aluminium silicate phosphors. Opt Mater (Amst) 58:234–242
22. Guo Q, Liao L, Mei L, Liu H (2015) Color-tunable photoluminescence and energy transfer properties of single-phase Ba<inf>10</inf>(PO<inf>4</inf>)<inf>6</inf>O:Eu^{2+}, Mn^{2+} phosphors. J Solid State Chem 232:102–107
23. Qi S, Huang Y, Tsuboi T, Huang W, Seo HJ (2014) Fluorosilicate apatites M 2 Y 3 [SiO 4] 3 F (M = Sr, Ba) suitable for white light emitting diodes. Opt Mater Express 4(2):5505–5510
24. Patterson AL (1939) The scherrer formula for X-ray particle size determination. Phys Rev 56(10):978–982
25. Tao SW, Irvine JTS (2000) Synthesis and ionic conduction of apatite-type materials. Ionics 6:389–396
26. Rakovan J. (2002) Growth and surface properties of apatite, no. 1977
27. Liu H, Liao L, zhang Y, zhou T, Guo Q, Li L, Mei L ((2017) Structure refinement and luminescence properties of a novel apatite-type compound. $Mn_2Gd_8(SiO_4)_6O_2$ .Dyes and Pigments 140:87–91
28. Xinghong Gong, Yanfu Lin, Yujin Chen, Z Huang, Y Huang, Zundu Luo (2005) Syntheses, structure , and characterization of crystal La6Ba4(SiO4)6F2,a promising Laser Host. 17:1135–1138
29. Meng FG, Zhang XM, Seo HJ (2012) Optical properties of Sm3and Dy3ions in Gd2MoB2O9host lattice. Opt Laser Technol 44(1): 185–189
30. Blasse G (1968) Energy transfer in oxidic phosphors. Phys Lett A 28(6):444–445
31. Lee GH, Kang S (2011) Studies in crystal structure and luminescence properties of Eu 3-doped metal tungstate phosphors for white LEDs. J Lumin 131(12):2606–2611
32. Tatu C (2013) Correlated color temperature determination for led modulesusing a digital color sensor. UPB Sci Bull Ser A Appl Math Phys 75(1):225–232
33. Zhang Z, Han L, Zhao Y, Wang L, Yang S, Chu X (2017) Synthesis and photoluminescence properties of ALa 9 (SiO 4) 6 O 2 : Eu 3 + (A = Li , Na) red phosphor. Mater Res Bull 94:147–153